

# Development and application of a new Mangrove Vegetation Index (MVI) for rapid and accurate mangrove mapping

Alvin B. Baloloy<sup>a,\*</sup>, Ariel C. Blanco<sup>a,b</sup>, Raymund Rhommel C. Sta. Ana<sup>a</sup>, Kazuo Nadaoka<sup>c</sup>

<sup>a</sup> Training Center for Applied Geodesy and Photogrammetry, University of the Philippines-Diliman, Quezon City, 1101, Philippines

<sup>b</sup> Department of Geodetic Engineering, University of the Philippines, Diliman, Quezon City, 1101, Philippines

<sup>c</sup> Department of Transdisciplinary Science and Engineering, Tokyo Institute of Technology, Tokyo, Japan

**KEY WORDS:** Mangrove index, mangrove extent, Sentinel-2, Landsat, vegetation mapping, Philippines

## ABSTRACT

Advancement in Remote Sensing allows rapid mangrove mapping without the need for data-intensive methodologies, complex classifiers, and skill-dependent classification techniques. This study proposes a new index, the Mangrove Vegetation Index (MVI), to rapidly and accurately map mangroves extent from remotely-sensed imageries. The MVI utilizes three Sentinel-2 bands green, Near Infrared (NIR) and Shortwave Infrared (SWIR) in the form | NIR-Green | / | SWIR-Green | to discriminate the distinct greenness and moisture of mangroves from terrestrial vegetation and other land cover. Spectral band analysis shows that the | NIR-Green | part of MVI captures the differences of greenness between mangrove forests and terrestrial vegetation. The | SWIR-Green | part of the index expresses the distinct moisture of mangroves without the need for additional intertidal data and water indices. The MVI value increases with the increasing probability of a pixel being classified as mangroves. Eleven mangrove forests in the Philippines and one mangrove park in Japan were then mapped using MVI. Accuracy assessment was done using field inventory data and high-resolution drone orthophotos. MVI have successfully separated the mangroves from other cover especially terrestrial vegetation, with an overall index accuracy of 92%. The MVI was applied to Landsat 8 images using the equivalent bands to test the universality of the index. Comparable MVI mangrove maps were produced between Sentinel-2 and Landsat images, with an optimal minimum threshold of 4.5 and 4.6, respectively. MVI can effectively highlight the greenness and moisture information in mangroves as reflected by its moderate to high correlation value ( $r=0.63$  and  $0.84$ ,  $\alpha=0.05$ ) with the Sentinel-derived chlorophyll-a ( $C_a$ ) and canopy water ( $C_w$ ) biophysical products. This study developed and implemented two automated platforms: an offline IDL-based 'MVI Mapper' and an online Google Earth Engine-based MVI mapping interface. The MVI implemented in Google Earth Engine was used in generating the latest mangrove extent map of the Philippines. Additionally, the application of MVI were tested to four additional mangrove forests in Southeast Asia: Thailand, Vietnam, Indonesia and Cambodia; and to selected mangroves forests in South America, Africa and Australia.

## 1. Introduction

Mangrove forests provides several ecosystem services and coastal area protection for the tropical and subtropical coastlines of the world (Veettil et al., 2019). It supports high floral and faunal biodiversity and provide a diverse range of goods to coastal communities. Despite their importance, mangrove forests continue to decline primarily due to anthropogenic causes. Over the past 50 years, approximately one-third of the world's mangrove forests have been lost (Clough 1993; Diop 1993; Spalding et al., 1997; Alongi, 2002) due to factors such as conversion to aquaculture (Primavera, 2000; Primavera, 2005; Farnsworth and Ellison, 1998), sea level rise (Crooks et al., 2011; Field, 1995), urban development (Romañach et al., 2018), overexploitation for timber (Kathiresan and Bingham, 2001) and natural disturbance including typhoons (Villamayor et al., 2016; Cahoon and Hensel, 2003) and increase in precipitation patterns and intensity (Field, 1995; Ellison, 2000). Mangrove extent monitoring is therefore significant to detect the historical and current distribution of mangroves as affected by these threats. Accurate spatial information of mangrove forest extent is essential for both land-use planning and natural resources management.

Remote sensing has been a popular tool used in mangrove forest mapping, allowing estimation and publication of global estimates (FAO, 2003; Spalding et al., 1997). It offers an inexpensive alternative to field-based techniques which are only practical at the local scale. Remote Sensing allowed scientists and planners to observe real changes in the areal extent and spatial pattern of mangrove forests over the years. In the Philippines, Long and Giri (2011) have mapped the spatial distribution and areal extent of the mangroves in year 2000 using Landsat data and Iterative Self-Organizing Data Analysis Techniques (ISODATA) clustering. They reported a nationwide baseline extent of 268,996 ha in 1990, 256,185 ha in 2000, and 240,824 ha in 2010, showing a downward trend with almost 11% decline. The Bureau of Forest Development, now known as Forest Management Bureau, provided an extent estimate from year 1969 to 1984. Larger mangroves areas were reported in earlier years between 1918 (450,000 ha) to 1968 (448,310) (PCAARD and L.M. Lawas, 1974) which have significantly reduced to 220,984 ha in 2016 as reported by Global Mangrove Watch. The decline was attributed to overexploitation in coastal villages as brought by industrial activities and conversion to agriculture (Primavera, 2000). There are discrepancies in the estimates from different references as different satellite data and processing methods were used. Most of these misclassifications were observed in the Landsat-based estimates, including mangroves classified as water within small mangroves stands (Ghandi and Jones, 2019; Long and Giri, 2011).

\* Corresponding author

New mapping techniques are still being developed due to the limitations observed from previous proposed methodologies. In supervised and non-supervised mangrove classification techniques, there is the challenge in collecting and selecting training data from remotely-sense images. Aside from selecting the most appropriate imagery, the classification method must be highly considered (Lu and Weng, 2007). The classification accuracy of different classifiers varies among different studies on mangrove vegetation mapping such as Maximum likelihood classification (MLC) versus Support Vector Machine (SVM) (Deilmai et al., 2014; Kanniah et al., 2015), Artificial Neural Network (ANN) and Random Forest (RF) versus MLC and SVM (Ma et al., 2017; Sikdar et al., 2016) and ISODATA versus MLC (Giri and Muhlhausen, 2008; Roslani et al., 2013). It is difficult to derive generalized research results due to differences in input data and study sites. Selection of region-of-interests (ROIs) are prone to biases and is affected by the user's skill in identifying mangroves versus non-mangrove pixels. Users are also limited by the capacity of the computers needed in performing the mapping operations, including the availability of enough memory and storage to handle big data and collection of satellite images. Research studies on simplifying mangrove mapping methodologies and implementing the workflow on automated and cloud-based mapping is still lacking.

Spectral indices used in mapping vegetation are called vegetation indices. These indices such as the normalized difference vegetation index (NDVI, Rouse et al., 1973), Soil Adjusted Vegetation Index (SAVI, Huete, 1988), and Leaf Area Index (LAI) can highlight plant intrinsic properties that are well related to leaf greenness and vigor. Each index has its specific expression which can represent vegetation properties better than using individual bands. However, these known indices are not specific for mangroves and cannot alone discriminate mangroves from terrestrial vegetation (Winarsro et al., 2014). Mangroves and dense terrestrial mangroves may generate the same NDVI values and thus, separating them from remotely-sense images is difficult unless additional input data will be introduced. Some studies utilized elevation data (Liu et al., 2008) and tasseled cap transformation (Razali et al., 2019; Zhang and Tian, 2013) to further improve the classification accuracy. To address the challenge in mapping mangroves with the vegetation indices, some researchers have proposed mangrove-specific vegetation indices using different inputs bands and satellite data. One of which is the Mangrove Index (MI) proposed by Winarsro and Purwanto (2014). It was first applied in Alas Purwo Mangrove area, Banyuwangi East Java Province, Indonesia utilizing both Landsat-8 Near Infrared (NIR) and Shortwave Infrared (SWIR) bands (see Table 1). The formula were tested on other data such as Landsat ETM+ by incorporating different multiplication factor as modified to the radiometric resolution of the data. The authors have used MI together with NDVI image to detect degraded and non-degraded mangroves sites. Similar NDVI and MI pattern indicates areas in good condition, while opposite pattern indicates a degraded one. In term of MI values, high values indicate healthy mangroves. The study acquired field survey data but the accuracy of delineating the mangroves using MI was not reported.

The Mangrove Recognition Index (MRI) (Zhang and Tian, 2013) was also developed for mangrove forest observation from space using multi-temporal Landsat TM images with different tide levels. Changes in the low tide and high tide conditions can result to variations in the spectral signature of mangrove vegetation (Zhang et al., 2017; Lin and Fu, 1995). MRI index considers these intertidal effects and is sensitive to the wetness, greenness, and change of greenness (Table 1). In the equation, the Green Vegetation Index (GVI) expresses the vegetation characteristics while the Wetness Index (WI) expresses canopy water information. GVI and WI are products of tasseled cap transformation which is an orthogonal transformation of the original remotely sensed data space to a new feature space. Limited test of this index in Beilunhekou National Reserve Area of China using TM data have demonstrated that MRI can effectively separate mangroves from non-mangrove forests with 93.19% user's accuracy. The  $|GVI_L - GVI_H|$  equation in the MRI formula generates higher values for mangrove vegetation due to the intertidal inundation in the coastal environment. Meanwhile, the sum of  $|WI_L + WI_H|$  is high for mangrove forests and low for non-mangrove vegetation. Larger MRI values indicate that the pixels correspond to mangrove cover while lower MRIs correspond to other land cover such as terrestrial vegetation, water and bare soil. The applicability of MRI to other mangrove areas is then limited by the availability of tidal data, as tide condition vary significantly within regions and across the globe. Site-specific moisture and vegetation information during the low and high tides are necessary but might be limited from remotely-sensed images. To address this limitation, a Combine Mangrove Recognition Index (CMRI) was proposed by Gupta et al., 2018. CMRI (Table 1) utilizes NDVI to express the presence of vegetation and normalized difference water index (NDWI) to express water information of mangroves without the need for specific tidal data. Since NDVI and NDWI are negatively correlated, subtracting these indices increases the upper and lower range of the CMRI output and further magnifying the distinct values of different land covers with almost similar spectral signatures. CMRI was then used as an input to a classification method done to separate the Landsat scenes into four classes: water, land, non-mangrove vegetation and mangroves. The CMRI-based method requires training data to generate the output maps. The authors compared the result from the CMRI-based classification with that of NDVI, SAVI, and Simple Ratio (SR) wherein better accuracy (73.43%) was obtained by using the proposed index. Aside from Landsat, a new Sentinel-2 based index called the Mangrove Forest Index (MFI) was proposed by Jia et al., 2019. The index utilizes the reflectance of red-edge bands of Sentinel-2 imagery which are sensitive to submerged mangrove forests. The results showed that the submerged mangrove forests could be separated from the water background in the MFI output image. The study emphasized the capability of the NIR and red-edge bands in discriminating between vegetation and water. The said index was designed based on the reflectance peak in the NIR spectral regions of green vegetation (Jia et al., 2019).

Hyperspectral imageries are also being used for mangrove mapping (Kamal and Phinn, 2011; Jusoff, 2006). The Mangrove Probability Vegetation Index (MPVI) was proposed by Kumar et al. (2019) using bands derived from EO-1 Hyperion data. The Hyperion is a space-borne hyperspectral sensor acquiring 70 bands in the VNIR sensor and 172 bands in the SWIR, providing a total of 242 wavebands with ~10nm bandwidth, and 30-m ground resolution (Green et al., 2003). The MPVI identifies the Hyperion image pixels corresponding to mangroves by calculating their correlation coefficients with a candidate mangrove spectrum (Table 1). Aside from MPVI, the same authors have also proposed the Normalized Difference Wetland Vegetation Index (NDWVI) using Hyperion bands: one SWIR band and one green band to discriminate mangrove from non-mangrove vegetation. Combination of different classifiers were used to identify the hyperspectral image data into mangroves and non-mangroves classes. Using MPVI

alone generated an overall accuracy of 73.98% while MPVI and NDWVI combined gave a higher accuracy of 85.01% (Kumar et al., 2019).

The previous mangrove indices reported different accuracy and advantages over the other. Mapping using MRI and MPVI still requires access to tide data and hyperspectral imageries, respectively, which may be a challenge in rapidly mapping mangroves in local and regional scales using free satellite imageries. The application of MI is more straightforward, but accuracy must still be explored including the application of the index to other satellite data such as Sentinel-2. The MFI was already tested for Sentinel-2 imagery using four spectral bands. The effectiveness of MFI was mainly validated between submerged mangrove forest and water, while its performance in discriminating mangrove from terrestrial forests was not yet examined. In the proposed MVI, the mangrove class will be discriminated against all land-use and land-cover present in a single tide Sentinel-2 image. NIR and SWIR are the commonly used bands among the previous indices. NIR band is an input to the MI and CMRI through the computation of NDVI. The ability of SWIR and green bands in delineating mangroves using the Hyperion-based MPVI was further explored through MVI, but the focus is shifted on the use of multispectral band spectral responses between mangroves and non-mangrove vegetation cover.

This study proposed a new simplified mangrove index, the Mangrove Vegetation Index (MVI) using the NIR, SWIR1 and green bands of Sentinel-2 to allow rapid and accurate mapping of mangroves without the need for complex classification techniques which maybe time-consuming and user-skill-biased. The index was designed by analysing the spectral signatures and characteristics of mangroves and non-mangroves datasets from different study sites in the Philippines and Japan. The index was formulated to capture the distinctive greenness and moisture content of mangrove pixels, discriminating them from non-mangroves and other non-vegetation cover such as bare soil, water, and built-up. The study then utilized MVI for nationwide mangrove mapping, and for mapping mangroves within and outside the Southeast Asia region. The MVI threshold were analyzed among land-cover and land-uses MVI values, and accuracy were computed using nationwide field-acquired mangrove inventory and drone data. MVI was then tested to Landsat bands having the same input bands (SWIR1, NIR and green) to determine the applicability and universality of the proposed index. Lastly, MVI-based mangrove mapping was automated using two platforms: an IDL-based MVI mapper for offline processing and Google Earth Engine (GEE) interface for rapid, accurate and large-scale mangrove extent mapping.

**Table 1.**

Existing mangrove mapping indices for separating mangroves from non-mangrove pixels. The band inputs and ratio differ between the indices and satellite image used. Most of the earlier indices were implemented using Landsat images.

Index Name	Author	Formula	Satellite Image Used
Mangrove Index (MI)	Winarso and Purwanto, 2014	$MI = (NIR - SWIR / NIR \times SWIR) \times 10000$	Landsat
Mangrove Recognition Index (MRI)	Zhang and Tian, 2013	$MRI =  GVI_L - GVI_H  \times GVI_L \times (WI_L + WI_H)$ where GVI - Green vegetation index; WI - Wetness index; Subscript L - at low tide; Subscript H - at high tide	Landsat
Combine Mangrove Recognition Index (CMRI)	Gupta et al., 2018	$NDVI - NDWI$ where NDVI is the Normalized Difference Vegetation Index and NDWI is the Normalized Difference Water Index	Landsat
Mangrove Probability Vegetation Index (MPVI)	Kumar et al., 2019	$MPVI = \frac{n \sum_{i=1}^n R_i r_i - \sum_{i=1}^n R_i \sum_{i=1}^n r_i}{\sqrt{n \sum_{i=1}^n R_i^2 - (\sum_{i=1}^n R_i)^2} \sqrt{n \sum_{i=1}^n r_i^2 - (\sum_{i=1}^n r_i)^2}}$ where n = total number of bands in the image, $R_i$ is the reflectance value at band i for a pixel of the reflectance image, and $r_i$ is the reflectance value at band i for candidate spectrum of mangrove forest.	EO-1 Hyperion
Normalized Difference Wetland Vegetation Index (NDWVI)	Kumar et al., 2017	$NDWVI = (R_{2203} - R_{559}) / (R_{2203} + R_{559})$	EO-1 Hyperion
Mangrove Forest Index (MFI)	Jia et al, 2019	$MFI = [(\rho_{\lambda 1} - \rho_{B\lambda 1}) + (\rho_{\lambda 2} - \rho_{B\lambda 2}) + (\rho_{\lambda 3} - \rho_{B\lambda 3}) + (\rho_{\lambda 4} - \rho_{B\lambda 4})] / 4$ where the $\rho_{\lambda}$ is the reflectance of the band center of $\lambda$ , and i ranged from 1 to 4; $\lambda 1, \lambda 2, \lambda 3, \lambda 4$ are the center wavelengths at 705, 740, 783 and 865 nm, respectively.	Sentinel-2

## 2. Data and methods

The first part of the methodology focuses on establishing the mangrove vegetation index by analyzing the varying spectral response of Sentinel-2 bands between the mangroves and non-mangrove pixels. The mangrove vegetation indices previously discussed were used as guide data for the analysis. Different combinations of the significant bands were tested, but this paper will focus on how the MVI was formulated. The MVI was then applied to Sentinel-2 imageries covering the selected mangrove sites (Figure 1). The MVI accuracy was assessed for each study site using field surveys and high-resolution orthophotos. The second part of the methodology includes the generation of mangrove extent maps for the whole Philippines using the cloud-based MVI mapper. The generation of two automated tools for MVI mapping will be discussed.

### 2.1 Study sites

Five major mangrove sites in the Philippines and one in Japan were selected as the study sites, namely (1) Coron-Busuanga, Palawan; (2) Puerto Princesa, Palawan; (3) Panay Island; (4) Eastern Samar Island; (4) Zambales-Bataan and (5) Fukido, Ishigaki, Japan. A total of twelve subsites within the major mangrove sites were chosen for output validation (Table 1). Palawan is an archipelagic province located in the central western part of the Philippines. The island trends northeast-southwest between the South China and Sulu seas. Palawan is the Philippines' 'last ecological frontier' housing a huge collection of unique and diverse fauna and

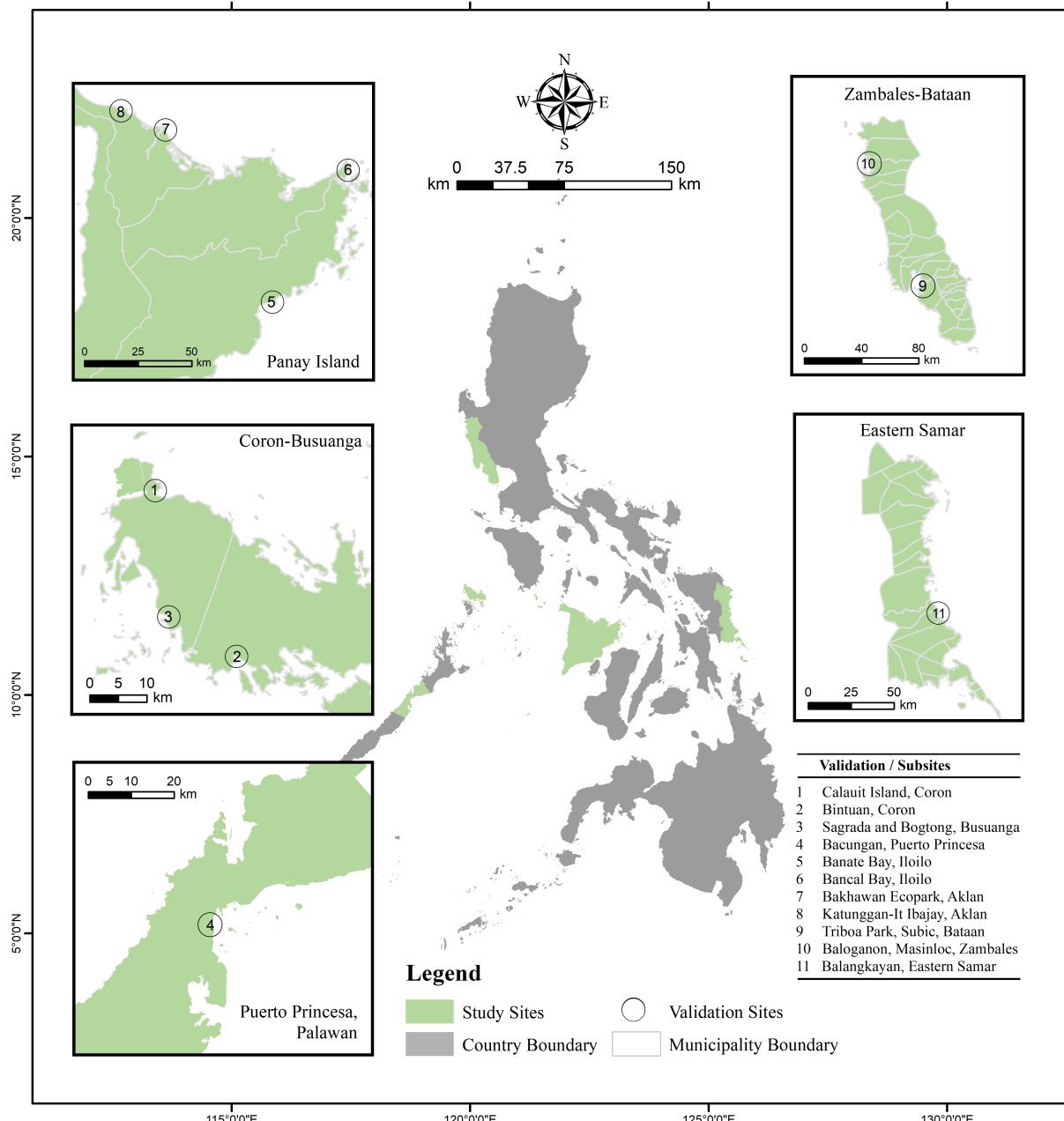


**Fig. 1.** Location of the major mangrove study sites (green) and the subsites in the Philippines where field data were collected. Coron-Busuanga, Puerto Princesa and Zambales-Bataan are located in Luzon, while Panay and Eastern Samar are in Visayas.

flora ([Sandalo and Baltazar, 1997](#)) including a total of 56,660 ha of mangroves ([Long & Giri 2011](#)). It consists of 23 municipalities including Coron and Busuanga; and one city, Puerto Princesa. Coron comprises the eastern half of Busuanga Island, all of Coron Island and about 50 other minor islets. Meanwhile, Busuanga covers the western one-third of Busuanga Island, as well as Calauit Island, which both are part of the Calamian Islands. Both sites have rich natural mangrove forests where two Marine Protected Areas (MPA) were declared: the Sagrada-Bogtong Marine Reserve in Busuanga and the Decalve Strict Protection Zone (Bintuan-Sangat Marine Park) in Coron ([Garces et al., 2012](#)). Puerto Princesa is a city in the province of Palawan, supporting 11.7% of the total mangroves in the island. There are 18 true and 20 associate mangrove species found in Puerto Princesa, mainly within the Honda Bay, Ulugan Bay, and Puerto Princesa Bay.

Panay Island is a triangular island located in the western part of the Visayas. It is divided into four provinces: Aklan, Antique, Capiz and Iloilo. Two known species-diverse mangrove ecoparks are found in Aklan in Northern Panay: the 45-hectare Katunggan-It Ibajay (KII) Ecopark and the 79-hectare Bakhawan Ecopark. In Iloilo, mangroves are dominantly distributed in the east coast of the municipality of Banate, facing the Banate Bay. Masinloc and Subic are the two subsites selected within Zambales and Bataan, two adjacent provinces in the island of Luzon. Masinloc is a coastal municipality in the province of Zambales with a reported mangrove extent of 109 ha, 36 % of which are old stands. Subic Bay Freeport Zone or Subic is a special economic zone covering portions of Olongapo City and the towns of Subic in Zambales and Morong and Hermosa in Bataan. It houses the Triboa Bay Mangrove Park, a two-hectare reforestation project.

Fukido Mangrove Park in Japan was added as an additional site for MVI validation. The Fukido Mangrove Park is located in the northeastern part of Ishigaki Island, southwest of Ryukyu Islands. This natural and estuary mangrove forest was designated as a national sanctuary by the Ministry of the Environment of Japan ([Sharma et al., 2014](#)). *Rhizophora stylosa* and *Bruguiera gymnorhiza* are the only dominant species in the mangrove park.

## 2.2 Satellite Data and Pre-processing

The Sentinel-2 Multispectral Imager Instrument (MSI) Level 1-C images covering KII Ecopark, Coron, Busuanga and Fukido Mangrove Park were downloaded from Sentinel Scientific Data Hub ([ESA](#)) (see Table 2). The product is already orthorectified, georeferenced, and radiometrically calibrated into top-of-atmosphere (ToA) reflectance data. Atmospheric correction was carried using Sen2Cor standalone tool, which can be processed alternatively in the S2A Toolbox of the Sentinel Application Platform (SNAP). This processor uses image-based retrievals with Look-Up tables (LUTs) pre-calculated from the libRadtran model to minimize or remove atmospheric effects from level 1-C images ([Main-Knorn et al., 2015](#)). All Level-2A bands were resampled to 10m pixel size using SNAP (ver. 5.0) geometric operation tool.

**Table 2.**

Date of field survey collection and the corresponding Sentinel-2 data used for each mangrove study sites and subsites

Study Sites	Coverage of Validation Data	Sentinel-2 Acquisition Date	Drone Survey / Field Inventory Date
Coron-Busuanga	Calauit Island	February 2017, 2018	July 2018
	Bintuan in Coron	February 2018	May 2018
	Sagrada and Bogtong in Busuanga	February 2018	May 2018
Puerto Princesa, Palawan	Bacungan	May 2018	October 2018
Panay Island	Banate Bay, Iloilo	August 2017	January 2018
	Bancal Bay, Iloilo	May 2019	January 2018
	Katunggan-It Ibajay, Aklan	February 2018	September 2018
	Bakhawan Ecopark, Aklan	August 2017	September 2018 / November 2017
Zambales-Bataan	Triboa Mangrove Park, Subic in Bataan	March 2018	August 2018
	Baloganon, Masinloc in Zambales	February 2016	November 2015
Eastern Samar	Balangkayan	June 2018	June 2019
Fukido, Ishigaki	Fukido Mangrove Park	February 2018	August 2018

Sentinel-2 images with the least cloud cover and at least close to the drone survey date were selected. A single Sentinel-2 tile may cover more than one subsite, such as the Path T50PRU covering Calauit, Bintuan and Sagrada-Bogtong in the Coron-Busuanga sites. Once resampled, the needed bands were stacked: from Blue (490 nm, Band 2), Green (560nm, Band 3) to NIR (842 nm, Band 8), NIR Narrow (865 nm, Band 8A), SWIR1 (1610 nm, Band 11) and SWIR2 (2190 nm, Band 12). MVI can already separate the mangroves from clouds and non-mangrove vegetation based on the threshold test. Selection of cloud-free Sentinel-2 images can significantly hasten the mapping time using MVI due to less noise pixels to be removed in the final output.

Landsat-8 scenes with minimum cloud cover for year 2017 were also obtained for MVI comparison. The data was downloaded from the USGS Landsat 8 Surface Reflectance Tier 1 dataset in Google Earth Engine. This dataset is already atmospherically

corrected surface reflectance using the LEDAPS software (Schmidt et al. 2013). The surface reflectance products have been atmospherically corrected using Land Surface Reflectance Code (LaSRC) algorithm which includes a cloud, shadow and water mask.

### 2.3 Formulation of MVI

#### 2.3.1 Sentinel-2 input bands

Based on related studies on mangrove vegetation properties and spectral responses within the spectral wavelengths, three multispectral bands were selected to be formulated into the MVI. These are the SWIR1, NIR (Band 8) and green (Band 3). The SWIR and NIR bands were found to be effective in characterizing water absorption in vegetation, and vegetation greenness, respectively (Manna and Raychaudhuri, 2018; Wang et al., 2018). Both SWIR1 and SWIR2 are affected by leaf liquid water. SWIR1 region is more useful in extracting vegetation information such as nitrogen compared to SWIR2 (Herrmann et al., 2010). High nitrate concentration in plants was found to increase root water uptake (Gorska et al., 2008), resulting to synergistic transport between nitrate and water (Tyerman et al., 2017). Although SWIR2 is useful for soil and vegetation unmixing, the spectral band needed to extract canopy moisture information for MVI must also be affected by the background soil moisture to help distinguish wet from dry vegetation. As seen in Figures 2-3, the difference in the canopy moisture-affected surface reflectance of mangroves and terrestrial vegetation are more distinguishable in the SWIR1 region. Meanwhile, the green wavelength region was found to be optimal for species discrimination in addition to the water absorption regions (Kumar et al., 2019; Prasad and Gnanappazham, 2015). The three bands were stacked into one data file and were imported to ENVI where MVI formula was applied.

#### 2.3.2 Development of MVI

The main test spectral bands in the formulation of the index was derived from the atmospherically corrected Sentinel-2 images acquired over the Coron-Busuanga site. This is due to the occurrence of various land-cover and land uses such as thick mangroves, sparse mangroves, forests and other terrestrial vegetation classes, built-up surfaces, water and bare soil. One hundred training data for each mangroves and non-mangroves vegetation classes were collected and the equivalent reflectance values in the green, NIR and SWIR1 wavelengths were analyzed (Figures 2-3). Vegetation types, either coastal or terrestrial, have higher reflected radiation in the NIR wavelengths than in visible wavelengths. Chlorophyll strongly absorbs visible light from 400 to 700 nm wavelength while cell structure of the leaves strongly reflects near-infrared light from 700 to 1100  $\mu\text{m}$  wavelength. Leaf pigments and cellulose are transparent to the NIR wavelengths resulting to high leaf reflectance (Huete, 2004). Among the visible spectrum, reflectance is highest in the green wavelength (Ashraf et al., 2011; Rullan-Silva et al., 2013). Smaller difference in the reflectance values between the visible regions reflects that the forest is sparse, while larger difference reflects that the forest is dense. Between forest types, however, there are distinct differences observed in the reflectance levels in the NIR and green regions when mangrove forest and terrestrial forest were compared.

The NIR reflectance of terrestrial vegetation could be either higher or lower than mangroves (Figure 2A). It is usually dependent on the health of the internal chlorophyll structure and leaf cellulose which reflect the near-infrared EM waves. Among the sample terrestrial vegetation data, lower reflectance in the green wavelength is observed when its reflectance in the NIR is lower, but not to the extent that it is lower than the green reflectance values of mangroves (Figure 2B, ‘sparse terrestrial vegetation’). Pixels selected within terrestrial forests classified as ‘dense terrestrial vegetation’ show high reflectance both in the NIR and the green regions of the spectrum. If we then subtract the green values from NIR, the difference will be always greater for mangroves compared to terrestrial vegetation classes.

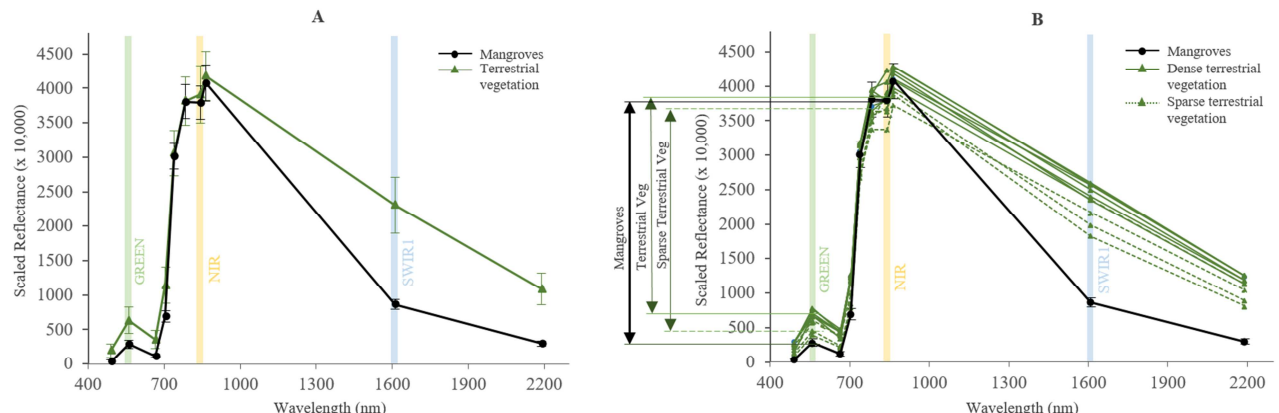


**Fig. 2.** Baseline theory based on the scaled spectral reflectance of mangroves and terrestrial vegetation (A) and mangroves, sample dense terrestrial vegetation and sparse terrestrial vegetation (B). The comparison focused on the reflectance values within the green (560 nm), NIR (842 nm) and SWIR1 (1,610 nm) of the Sentinel-2 image, where lower reflectance values of mangroves in the green and SWIR regions were observed compared to reflectance values of either dense or sparse vegetation. The reflectance in the NIR regions varies, but the difference of the reflectance values between the NIR and green regions in the terrestrial vegetation is always smaller than the difference observed in mangroves.

In some cases, there are vegetation types including very dense trees within closed forests and wet dense grass with relatively higher NIR values than mangroves (Figure 3) that may produce very small to negligible difference if only the first baseline theory (Figure 2) will be considered. Thus, there is a need for additional observation to discriminate these types of vegetation from mangroves. It was observed that non-mangroves vegetation with high reflectance in the NIR wavelength also have higher SWIR values than those of mangroves (Figure 3). If we then subtract the green values from SWIR, the difference will be always smaller for mangroves. The leaves and canopies of mangroves contains higher water content in comparison to most of the terrestrial vegetation (Kumar et al., 2019; Tomlinson 1994). The reflectance of mangroves in the SWIR1 spectrum is also lower due to presence of moist soil as affected by tide inundation. This is clearly visible in Figure 3 where the scaled reflectance values of mangroves is below 1000.

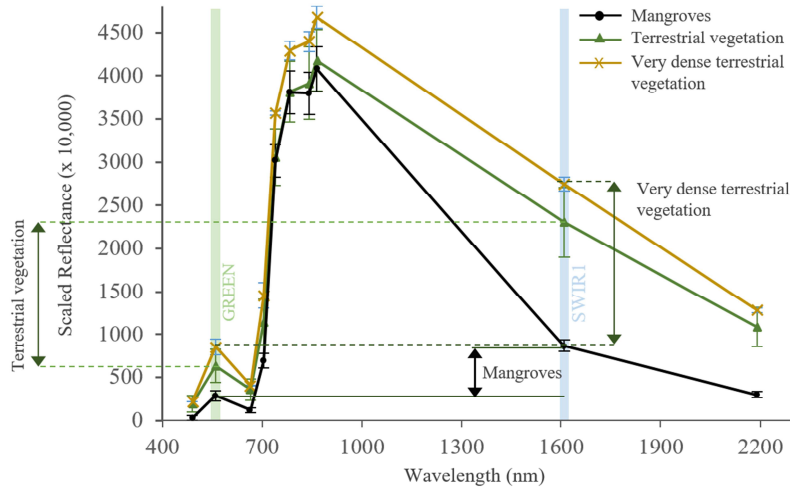


**Fig. 3.** Baseline theory based on the spectral reflectance of mangroves, terrestrial vegetation and very dense terrestrial vegetation, showing the extent of the reflectance differences between the SWIR1 and green regions of each class. The difference between the SWIR and green values for mangroves is relatively smaller than the difference observed in the same spectral regions of sparse to dense and very dense terrestrial vegetation. Very dense vegetation pixels commonly have high SWIR values, making it separable from the mangrove pixels.

The two main observations were considered into the Mangrove Vegetation Index (MVI) equation:

$$\text{MVI} = (\text{NIR} - \text{Green}) / (\text{SWIR1} - \text{Green}) \quad (1)$$

where NIR, Green, and SWIR1 are reflectance values in Sentinel-2's band 8, band 3, and band 11, respectively. The first part of the equation | NIR-Green | enhances the differences of vegetation greenness between mangrove forests and terrestrial vegetation; while the second part of the equation | SWIR1-Green | expresses the distinct moisture of mangroves due to its environment. MVI measured the probability of mangrove pixels by utilizing the green, NIR and SWIR1 bands to highlight mangroves' greenness and moisture, separating it from other classes especially from terrestrial vegetation. Higher quotient reflects higher probability of a pixel being a mangrove. Minimum and maximum MVI thresholds were set using sparse and dense mangrove data. Although the difference of red band and NIR is larger than the difference of the green band and NIR (Figure 3), the gaps in the spectral signature of mangroves and terrestrial vegetation classes are larger and more distinguishable in the green region (SD = 286) than in the red region (SD = 153). The larger the spectral gap, the larger will be the difference in the MVI dividend between the mangrove and non-mangrove classes which will be useful in separating the mangroves.

### 2.3.3 MVI Threshold

Training samples were selected from a Sentinel-2 image containing different land-use and land cover. Each of the training pixels represents pure sample of the selected class. The spectral signatures of the selected pixels were checked prior to MVI generation. Mean, upper and lower thresholds of mangroves and non-mangroves were identified by generating the MVI for the following classes: mangroves, terrestrial vegetation (forest and non-forest), bare soil, built-up, water and clouds.

### 2.4 Application of MVI to Sentinel-2 Images

Atmospherically corrected Sentinel-2 images covering the six major sites were used as inputs for the index computation (Figure 4). All bands were resampled to 10m resolution and were stacked as one file. The MVI formula was applied to the stacked images using ENVI 5 band math tool. The MVI outputs were then filtered to select only the pixels within the mangrove MVI values based on the identified threshold value. Each filtered mangrove MVI raster covering the sites was converted into shapefile. Cleaning of noise pixels, if applicable, were applied by overlaying the shapefile to the false-color Sentinel-2 image.

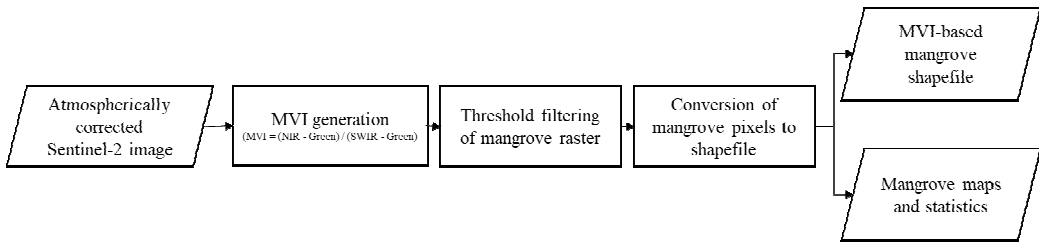


**Fig. 4.** Workflow used in generating the MVI-based mangrove maps from Sentinel-2 imagery. Atmospherically corrected image was used as inputs where the green, SWIR1 and NIR bands were utilized in generating the MVI output image in ENVI 5. Threshold selection is a significant step to separate the mangrove MVI pixels from the other classes. The filtered mangrove output was exported in ArcGIS software to facilitate noise pixels deletion, map layout and statistics computation.

## 2.5 Index Accuracy Assessment

A total of 2,727 validation pixels were used in the study from mangrove field inventory and high-resolution drone orthophotos as reference maps. The accuracy was computed by calculating the validation pixels that were correctly mapped in the MVI outputs. For a single subsite with both field inventory and drone data available, the mean accuracy between the two data was used.

**Table 3.**

Source of validation data and total number of validation pixels for the twelve subsites to assess the accuracy of the generated MVI maps. Geotagged mangrove location from field inventory and randomized points selected within the drone-acquired orthophotos were the main validation data used in this study. The overall accuracy was then computed from the average accuracy of the subsites.

Study Site	Coverage of Validation Data	Validation Data	Total Validation Pixels
Coron-Busuanga	Calauit Island	Drone orthophoto	50
	Bintuan (Coron)	Drone orthophoto	50
	Sagrada and Bogtong (Busuanga)	Drone orthophoto	50
Puerto Princesa, Palawan	Bacungan	Drone orthophoto	50
Panay Island	Banate Bay, Iloilo	Drone orthophoto	50
	Bancal Bay, Iloilo	Drone orthophoto	50
	Katunggan-It Ibajay, Aklan	Drone orthophoto	50
Zambales	Bakhawan Ecopark, Aklan		90
	Triboa Mangrove Park, Subic	Drone orthophoto	15
	Baloganon, Masinloc	Field inventory data	2,148
Eastern Samar	Balangkayan	Drone orthophoto	50
Fukido, Ishigaki	Fukido Mangrove Park	Drone orthophoto and field inventory data	74

Most of the field inventory data contain information on the mangrove tree location, the species name, and tree height. These mangroves were selected and GPS-tagged on site to collect representative tree sample for each species present, regardless of the zonation, vegetation density, and distance from the shore. For the purpose of the study, only the mangrove location is needed. Higher validation samples were obtained from Masinloc due to an existing plot-level field inventory data. The drone photos within the subsites were acquired using DJI Phantom 3, DJI Phantom 4, and Sensefly eBee drones mounted with either RGB or Sequoia multispectral camera. The generation of orthophotos was carried in Pix4D software. The spatial resolution of the orthophotos varies from 3 to 5cm, high enough to be used as validation data.

## 2.6 Application to Landsat OLI

The bands needed to generate an MVI from Sentinel-2 imagery are also present in Landsat. Bands 3, 5, and 6 are the equivalent green, NIR and SWIR1 bands in Landsat-8, as seen in the formula below and in Table 4. Landsat SWIR1 (Band 6) was selected over SWIR2 (Band 7) to generate comparable results with Sentinel2-based MVI which also utilizes SWIR1 (Band 11). Both are within similar wavelength range, from 1565 nm to 1655 nm. The spectral wavelength comparison between the two sensors is shown in Table 4.

$$\text{Landsat-8 MVI} = (B5 - B3) / (B6 - B3) \quad (2)$$

$$\text{Sentinel-2 MVI} = (B8 - B3) / (B11 - B3) \quad (3)$$

The threshold for Landsat8-based MVI was identified using the atmospherically corrected Landsat image covering Calauit, Busuanga. Visual variations of the output MVI mangrove maps from the two satellite data were examined. In addition, correlation between Landsat and Sentinel MVI input bands were analyzed to understand the similarities or differences between the output MVIs.

**Table 4.**

MVI input bands and the corresponding band wavelengths for Landsat-8 OLI and Sentinel-2.

Multispectral band	Landsat-8	Sentinel-2		
	Band No.	Wavelength (nm)	Band No.	Wavelength (nm)
Green	B3	533 - 590	B3	543 - 578
NIR	B5	851 - 879	B8	785 - 900
SWIR1	B6	1,567 - 1,651	B11	1565 - 1655

## 2.7 Comparison with Vegetation and Biophysical Indices

The correlation of MVI with NDVI, LAI and fractional vegetation cover (FVC) were examined. LAI and FVC were generated from the atmospherically corrected and resampled (10m) Sentinel-2 data using the biophysical processor toolbox of SNAP. These products are outputs of tested, generic algorithms based on specific radiative transfer models. The generation of LAI and FVC were composed of three main steps: (1) normalization of the inputs, (2) implementation of the artificial neural network (ANN) algorithm, (3) denormalization of the output and (4) generation of quality indicator ([Weiss, 2016](#)). The comparison and analysis of MVI with LAI and FVC were employed using mangrove pixels obtained from two forest types with different greenness and moisture characteristics: riverine and fringe mangrove forests. Index correlation and map comparison were done. The efficiency of MVI in determining mangrove health was tested by comparing it with the NDVI, LAI and FVC values within the two forest types. In addition, Sentinel-2 derived chlorophyll-a ( $C_a$ ) and canopy water ( $C_w$ ) were generated from SNAP to determine their correlation with MVI. The  $C_a$  and  $C_w$  are two readily available Sentinel-2 biophysical products for canopy greenness and canopy moisture analyses.

## 2.8 Automation of MVI

To facilitate faster processing especially for large-extent mangrove mapping, a sub-automated workflow and an automated workflow were designed which can be respectively implemented offline and online. The first one is an IDL-based ‘MVI Mapper’ tool was developed for offline semi-automated processing. For fully automated processing online, the MVI Mapper was also implemented in Google Earth Engine.

### 2.8.1 IDL-based Offline MVI Processing

The *IDL*, short for Interactive Data Language, is a program language widely used in astrophysics which is mainly for data analysis and visualizations of complex numerical data. IDL consists of both an interactive programming environment and a programming language, its main advantage over other languages ([Bowman, 2004](#)). Since IDL is a commercial software, the IDL used in the study is the version included in the ENVI 5 package (IDL v. 8.5). The MVI script is called the ‘MVI Mapper’ which was developed as guided by the initial workflow (Figure 4). The non-automated component includes the downloading of Sentinel-2 image from either Earth Explorer or Sentinel Scientific Data Hub, and atmospheric correction and resampling in SNAP software. The automated MVI script facilitates the processes of MVI image generation, image masking using the user-selected threshold, and generation of MVI vegetation raster, mangrove raster and mangrove shapefile.

The MVI mapper will initially require users to input the directory of the resampled atmospherically corrected data and the desired output folder directory. The mapper will then proceed to the generation of MVI images based on the inputted threshold. Total time of processing for the selected sites were recorded. The IDL based methodology were mainly utilized if the satellite data were already pre-downloaded or available. It can be used in any computers with an IDL software installed, without the need for internet connection as the IDL workflow runs offline. In the case of the nationwide mangrove mapping, the IDL based method will still consume some time for data download.

### 2.8.2 Google Earth Engine-based MVI Mapping

An online MVI mapper was developed for larger extent mangrove mapping where manual satellite download and pre-processing is not needed. The workflow is fully automated, from the sourcing of atmospherically corrected Sentinel-2 (Level-2A) input from Google Earth image database to the generation of four products: RGB and false color composite images, MVI vegetation raster and MVI mangrove raster. A graphical user interface (GUI) was further developed for user-friendly processing. The MVI mapper requires users to input the desired Sentinel-2 tile, the start and end date, the lower and higher MVI mangrove threshold, and the selected outputs from a list of products, including RGB and false color composite images, MVI vegetation raster and MVI mangrove raster. False color composite and RGB images were included as outputs to aid in the quality assessment of the generated mangrove raster. The conversion of MVI raster to shapefile is done outside the GEE where data cleaning is possible.

## 2.9 Generation of nationwide MVI-based mangrove maps

The MVI was initially applied to the six study sites consist of twelve subsites, eleven of which are in the Philippines. The GEE-based MVI Mapper was utilized to generate an updated nationwide mangrove maps using Sentinel-2 images acquired within year 2019. Available 2016 mangrove map from Global Mangrove Watch was used to determine the needed Sentinel-2 tiles to be included in the processing. A total of 106 tiles were detected. The mangrove MVI raster outputs were downloaded and quality-checked in ENVI software. The raster images were converted to shapefiles in ArcGIS. In some images with noise pixels, false color composite

images were overlaid to aid in data cleaning. The total area of mangroves per tile was computed, which was further used in calculating the current mangrove extent in the country.

### 2.10 Generation of MVI for selected countries in Southeast Asia

The MVI was initially tested in a Sentinel-2 image covering Ishigaki, Japan as one of the study sites. The IDL-based MVI Mapper was also applied in generating the mangrove maps of other selected countries including Indonesia, Cambodia, Thailand, and Vietnam. The purpose of this is to test the applicability of MVI in mapping mangroves in different mangrove forest types and mangrove zones. For each country, the false color image composite was used to determine the specific Sentinel-2 tiles with mangrove cover. The map outputs for the said countries were compared with previous mangrove extent estimates.

### 2.11 Application to Mangrove Forests outside Asia

Three additional mangrove sites were added to test the applicability of the MVI for mapping mangroves outside Asia. The mapping threshold, greenness and moisture characteristics were compared between mangrove forests. These sites are Baía de São José, Amazon Coast in Brazil, Mabokweni in Tanzania, and Prince Regent National Park in Western Australia. These are representatives of mangrove forests located in three different continents: South America, Africa, and Australia, respectively, with varying substrates, mangrove types, and mangrove ecosystem characteristics.

### 2.12 Index Uncertainties due to Tidal Level and Rainfall

Three subsites were selected to determine the effect of tidal level and precipitation to the MVI metrics, including mangrove area and mean mangrove MVI value. These are Bintuan in Coron, Sagrada in Busuanga, and Pilar in Siargao. The Coron and Busuanga sites are located in the western region of the country with West Philippine Sea to the west and Sulu Sea to the southeast. The Siargao site was selected to represent an area located in the eastern region, facing the Pacific Ocean to the east. Sentinel-2 images acquired within different months and season of 2019 and early 2020 were used for this section. For Coron and Busuanga, the data downloaded were acquired January 8, 2019 (dry season); June 12, 2019 (wet season); December 29, 2019 (end of wet season); and January 23, 2020 (dry season). For Siargao, the data were acquired February 21, 2019 and August 10, 2019 for the dry and wet season, respectively.

Mangrove area and mean mangrove MVI value were computed for each satellite data based on the optimal minimum MVI threshold needed to separate the mangroves. The variation in the MVI products were explored through comparison with precipitation and tidal data which may exhibit monthly and seasonal changes. The tidal data was acquired from WXTide32 Version 4.7 software ([Hopper, 2007](#)) specifically for 10:20 AM timestamp to be similar with the time of satellite acquisition. The tide stations used are Coron, Busuanga Island located 120°12.00 'E, 12°1.00 'N, and Pilar, Siargao located 120°6.00 'E, 9°52.00 'N. The default offset values for tide height measurement from the selected reference stations were used. The daily precipitation data was acquired from NOAA National Centers for Environmental Prediction (NCEP) Climate Forecast System Reanalysis dataset (CSFR) with 19.2-km grid resolution downloaded from <https://app.climateengine.org/climateEngine>. The total precipitation on the day of satellite acquisition and on three days earlier was included as one of the meteorological metrics. Moreover, the mean values of FVC, C<sub>w</sub>, NIR, and SWIR within the mapped mangrove areas were computed to better understand the MVI results. FVC and C<sub>w</sub> were generated using the same methodology discussed in section 2.7.

## 3. Results and Discussion

### 3.1 Mangrove Vegetation Index

The proposed MVI utilized three spectral bands, namely, SWIR1, NIR, and green, or bands 11, 8 and 3, respectively, in the case of Sentinel-2 (Equation 1). The SWIR band is commonly used in characterizing water absorption characteristics in vegetation ([Manna and Raychaudhuri, 2018](#)). It was observed by Winarso and Purwanto (2014) as an effective band in their mangrove index (MI) where it expresses the absorption of electromagnetic wave as affected by tidal-caused wet soil. SWIR bands were said to be significant for mangrove extent classification, then followed by the NIR band ([Wang et al., 2018](#)). NIR was selected as target input band due to its ability to express vegetation greenness. It was reported to be the spectral region where mangroves recorded the highest reflectance in sample hyperspectral images ([Basheer et al., 2019](#)). Reflectance of mangroves also differs among the bands in the visible region, although the difference in the spectral curve between most mangrove species are reported to be small ([Kamaruzaman and Kasawani, 2007](#)). The reflectance is lower in both the blue and the red regions of the spectrum due to its absorption by chlorophyll for photosynthesis (Figures 2-3). Combinations of SWIR1, NIR and green bands resulted to the MVI.

The proposed index is the first mangrove index to utilize green, NIR, and SWIR1 in a single equation, in contrast with the derived NDVI and NDWI indices used in generating CMRI ([Gupta et al., 2018](#)). With these bands, the MVI formula reflected two main properties of mangrove vegetation: greenness and moisture. MVI allows the calculation of ratio between the greenness and moisture resulting to values distinct to mangrove classes. Figure 3 have shown that the MVI values can already discriminate mangrove from non-mangroves vegetation, regardless of the density of terrestrial vegetation cover. In comparison with NDVI, LAI and other vegetation indices, MVI values are high for mangrove vegetation only and thus can be utilized as a single input for index-based mangrove mapping. Previous works reported the need to still combine the common vegetation indices such as NDVI, SR and SAVI to obtain higher accuracy in mangroves ([Alsaideh et al., 2013; Kongwongjan, et al, 2012](#)).

### 3.2 MVI Threshold

The MVI values of pixels identified as mangroves, terrestrial vegetation (forest and non-forest), bare soil, built-up, water and clouds were plotted in Figure 5. A total of 50 pure training samples were collected for each land cover class. For mangroves, training samples were chosen to represent all types of pure mangroves, ranging from sparse to dense cover, and from fringe to riverine mangrove forests. The mean mangrove MVI values is 7.7, with maximum value of 16.5 and minimum value of 4.5. The whole extent of this threshold is separated from the threshold of terrestrial forest and non-forest vegetation, with maximum threshold up to 3.6 only. This is the result of the distinct spectral response of mangroves in the green, NIR and SWIR1 wavelengths. To generate higher MVI values, the dividend (NIR-green) must be large while the divisor (SWIR-green) must be small. In terms of terrestrial vegetation, its reflectance in the NIR region could be higher than mangroves but subtracting its reflectance values in the green region from that of NIR made the MVI dividend smaller.

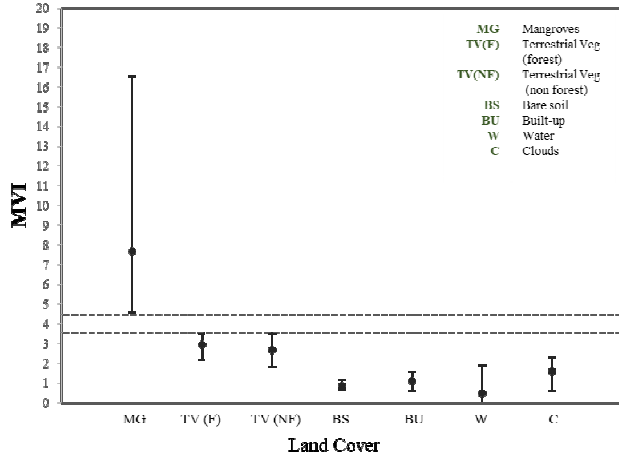


**Fig. 5.** Mean, maximum and minimum MVI values of mangroves and non-mangroves classes: terrestrial vegetation-forest (TVF), terrestrial vegetation- non forest (TVNF), bare soil (BS), built-up (BU), water (W) and clouds (C). The minimum threshold for mangrove MVI was observed to be 4.5, higher than the maximum MVI values of terrestrial vegetation (3.5). Clouds, water, built-up and bare soil generated lower MVI values than the vegetation classes due to differences of spectral reflectance in the green, NIR and SWIR bands. The lowest MVI was recorded for water due to its high absorption in the three spectral regions used for MVI.

The SWIR1 values of terrestrial vegetation is also higher than mangroves, while the SWIR1 values of mangroves is usually low due to incident radiation absorption by leaf water. The SWIR1 and NIR values of terrestrial forest is lower than the terrestrial non-forest vegetation (Figure 6). MVI, similar with other mangrove indices, is well dependent on the moisture information of mangrove pixels as affected by its coastal habitat (Zhang and Tian, 2013). The proposed index assumes that coastal wetland conditions can already be reflected by the SWIR1 values, mainly due to the leaf water content (Huete, 2004) and background reflectance of soil and water. Canopy water content of mangroves increases with increased salinity (Nguyen et al., 2017) and high humidity levels because of tidal inundations (Al-Saidi et al., 2009), factors that are common in a mangrove environment. Some uncertainties in this assumption will be discussed later in section 3.12.

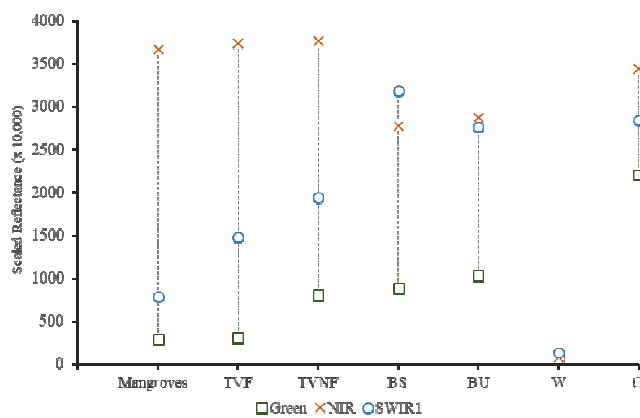


**Fig. 6.** Scaled reflectance values of mangroves, terrestrial vegetation-forest (TVF), terrestrial vegetation-non forest (TVNF), bare soil (BS), built-up (BU), water (W) and clouds (C) in the green (560 nm), NIR (842 nm) and SWIR1 (1,610 nm) regions. By disregarding the water class, the lowest green and SWIR1 reflectance values were obtained with mangroves, while the terrestrial vegetation classes registered higher green values than mangroves.

The MVI values of bare soil and built-up ranges from 0.65 to 1.15 and 0.6 to 1.57, respectively (Figure 5). Soil (BS) and built-up (BU) both have high reflectance values within the NIR and SWIR1 regions (Figure 8). The SWIR1 reflectance of soil is highly dependent on the mineral, organic matter and water content at the surface (Cierniewski and Kuśnerek, 2010; Huete, 2004). High

reflectance of built-up in SWIR1 region is mainly driven by urban surfaces and man-made materials. With high NIR and low green reflectance values, the MVI formula dividends for soil and built-up classes are high. However, the MVI divisor is also high due to high reflectance in the SWIR1 region, to be subtracted by low reflectance values in the green region. The resulting MVI values are relatively lower than mangroves MVI, as shown in Figure 5. The reflectance of water (W) is low in all spectral regions especially in the NIR (Figure 6) due to its high absorbing properties.

The 4.5 threshold for extracting mangrove pixels was applicable to the eleven subsites used in this study. In the case of small mangroves located in drier locations such as the Triboa site (2 ha), the threshold was adjusted to a lower value of 3.5. The said threshold can already separate the mangroves from the terrestrial vegetation, which also have lower MVI values in Triboa compared to the terrestrial vegetation within the other sites. It was previously observed that the SWIR1 value of mangroves increases as the leaf water content decreases (Huete, 2004; Tucker 1980), which can lessen the output MVI values. The reflectance of mangrove in the visible regions, on the other hand, is not responsive to the factors affecting canopy moisture such as tidal inundation (Huete, 2004).

### 3.3 Generated MVI Images

Sentinel-2 images covering the six study sites (Table 3) were used in generating the MVI bands. Comparison of the false color composites and the MVI products for the Philippine sites are shown in Figures 7 to 9. Clear delineation of mangroves was observed especially in Busuanga (Figure 8), Coron (Figure 9-A) and Calauit Island (Figure 9-B) where large mangrove covers exist.

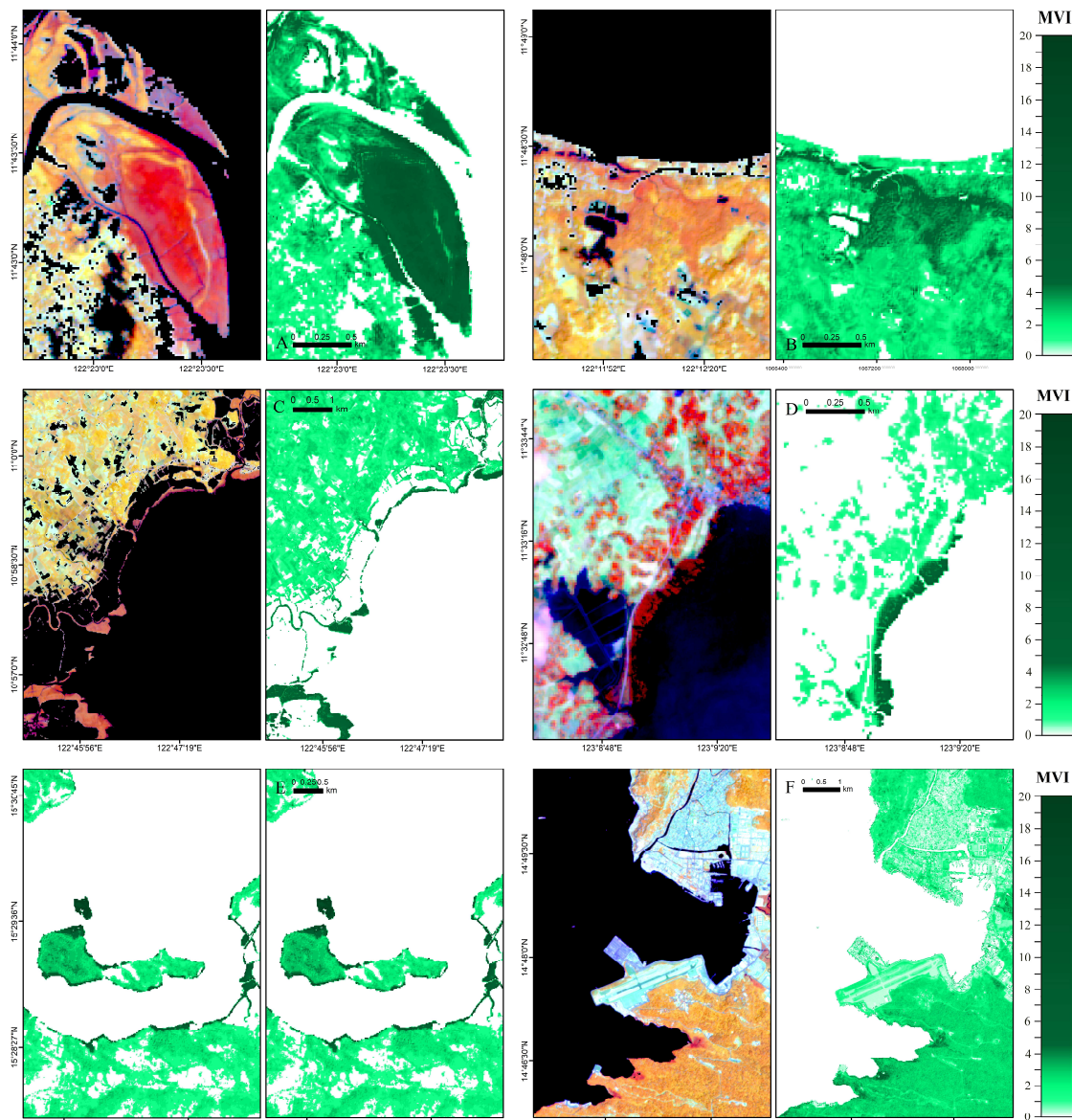


**Fig. 7.** False color composite (RGB B11-B8-B4) visualization of the atmospherically corrected Sentinel-2 images and the output MVI images in the study sites: (A) Bakhawan Ecopark, Aklan, (B) Katunggan-It Ibajay Ecopark, Aklan, (C) Banate Bay, Iloilo, (D) Bancal Bay, Iloilo, (E) Masinloc in Zambales and (F) Triboa Mangrove Park, Subic in Bataan.

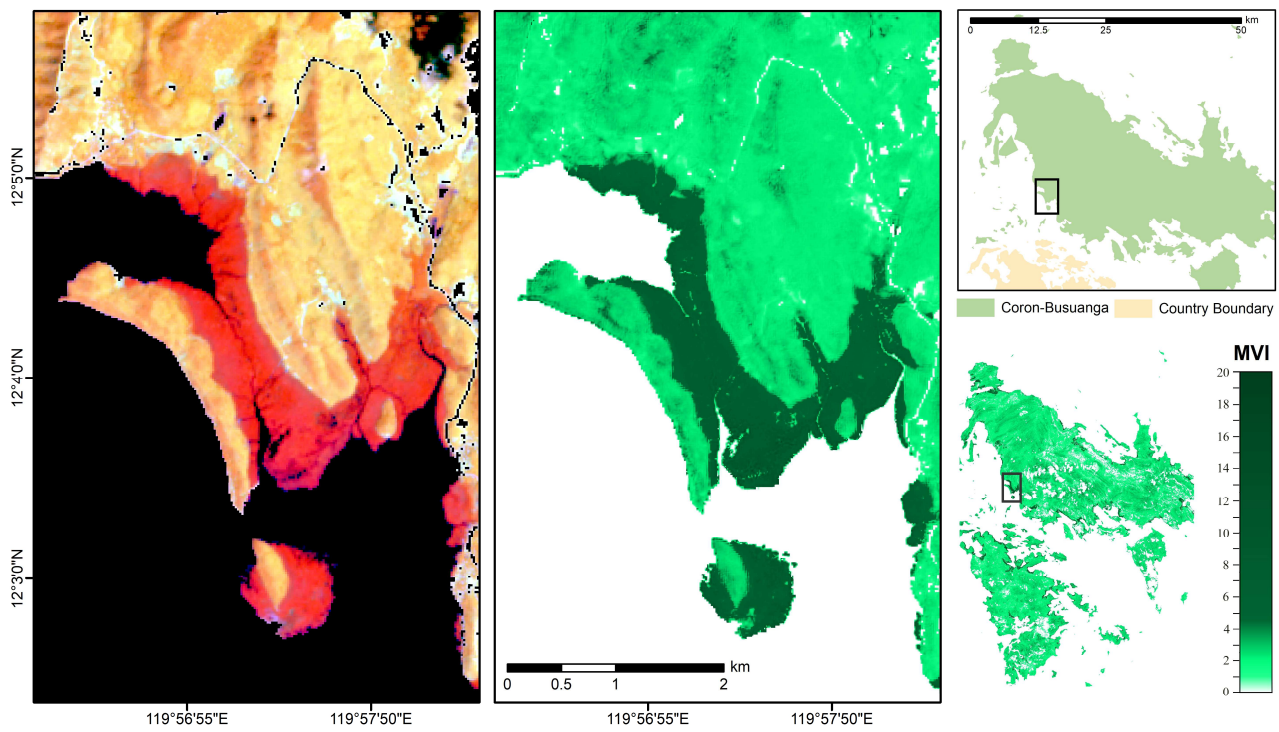


**Fig. 8.** Comparison of the false color (RGB B11-B8-B4) visualization of the atmospherically corrected Sentinel-2 image (leftmost) and the output MVI image (center) in Busuanga. The mangroves are in dark green color while the non-mangroves are in white to lighter green. The MVI clearly delineated both the nearshore and upstream mangroves by a threshold of 4.5.

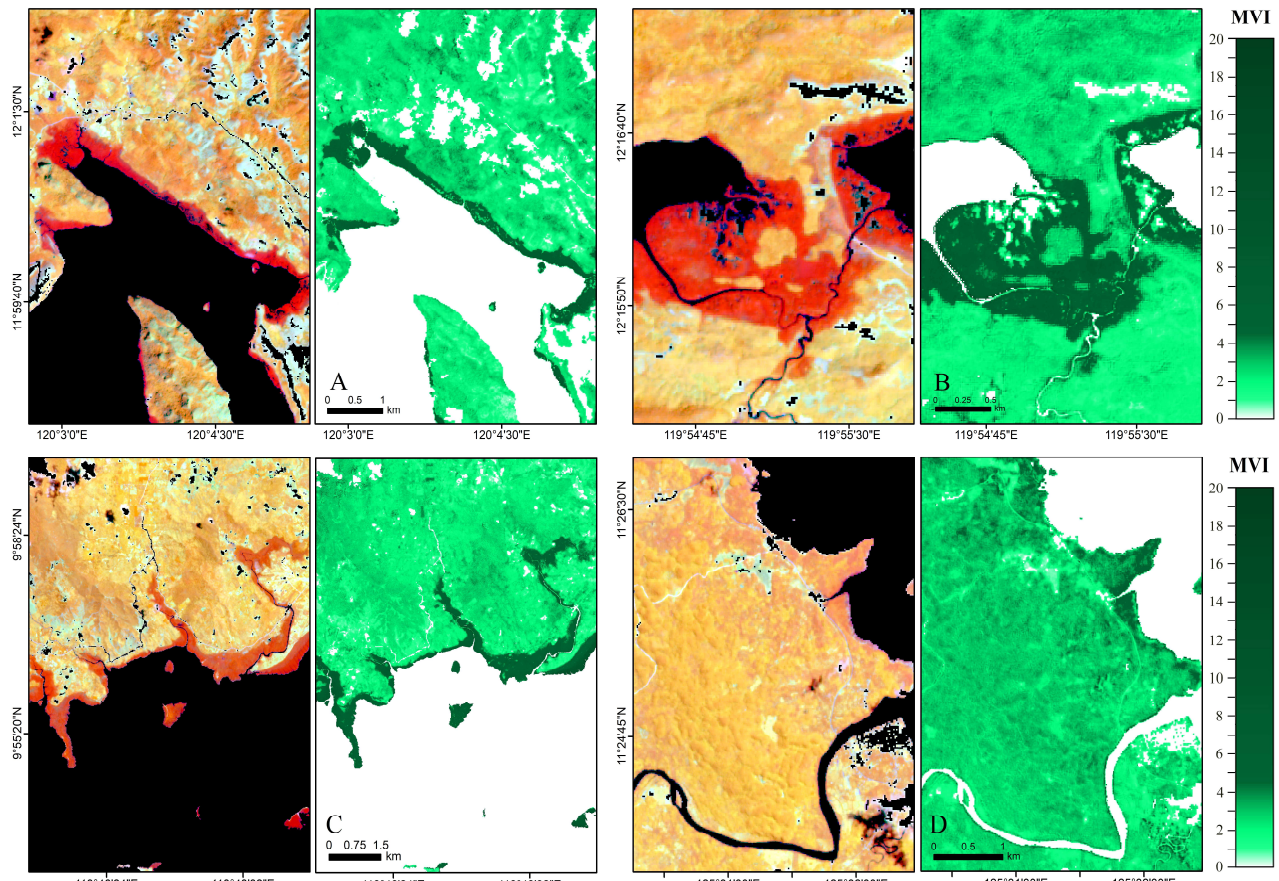


**Fig. 9.** False color composite (RGB B11-B8-B4) visualization of the atmospherically corrected Sentinel-2 images and the output MVI images in: (A) Bintuan, Coron, (B) Calauit, Busuanga, (C) Bacungan, Puerto Princesa, Palawan and (D) Eastern Samar.

Dense terrestrial vegetation situated in the northern part of Coron and Calauit generated lower MVI values, discriminating it from the mangroves. Most of these vegetation areas are located within dense closed forests. Inland water was successfully separated from the mangrove cover in sites including Calauit Island (Figure 9-B), Bacungan, Puerto Princesa, Palawan (Figure 9-C), and Bakhawan Ecopark, Aklan (Figure 7-A), although some water pixels were already masked out in the pre-processing steps. Some of these inland water areas were reported to be misclassified as ‘mangroves’ in previous mapping works (Bunting et al., 2018; Long and Giri, 2011). This was observed when the MVI-based map and the Global Mangrove Watch data of Calauit Island were compared, with only the earlier delineated the inland water from the actual mangrove cover, with water MVI values lower than 4. The Global Mangrove Watch (GMW) utilized mangrove masks based on the mask data of Giri et al. (2011) and Spalding et al. (2010) while the water occurrence layer was sourced from Pekel et al. (2016). Pekel’s water masks used by GMW has a spatial resolution of 30m while the initial water mask used in this study is 10m as derived from the resampled Sentinel-2 images. Since mangrove forests are located near the shoreline and therefore periodically submerged by tides, distinction between mangrove and water pixels could be affected by the time of satellite acquisition. Discriminating submerged mangrove from water background was previously performed using an index dependent on the reflectance peak in the NIR spectral regions (Jia et al., 2019), while the proposed MVI relies on the coupling responses of NIR and SWIR1 with the green wavelength among vegetation and water pixels. Other indices utilize NDWI as an input to separate water classes (Gupta et al., 2018). Thin mangrove forests such as those located in Banate Bay, Iloilo, (Figure 7-C) and Masinloc, Zambales (Figure 7-E) were correctly mapped using MVI. Sentinel-2 10m spatial resolution allows finer delineation of these mangroves near the coastline and along the river delta. Small patches of mangrove can still be detected, which is inadequate when a coarser satellite such as Landsat is used (Hoa and Binh, 2016). To consider the accuracy in delineating patches of mangroves, some of the validation points were selected from small and sparse cover.

The Japan study site is the Fukido Mangrove Park in Ishigaki Island. This site is relatively smaller than the Philippines sites, with two dominant species namely, *Rhizophora stylosa* and *Bruguiera gymnorhiza*. The total mangrove area estimated using MVI for the entire Ishigaki Island is 87 ha. This is close to the previously estimated area of 80 ha (Alsaadieh et al., 2003) and 100 ha (Ministry of Environment Reference Map). The drone and mangrove inventory both gave an accuracy of 92%.

### 3.4 Index Accuracy

Selected mangrove drone orthophotos used in validating the accuracy of the MVI maps are shown in Figure 10. These orthophotos have a spatial resolution of 3 to 5 cm. Multiples flights were conducted in areas with more than one subsite.

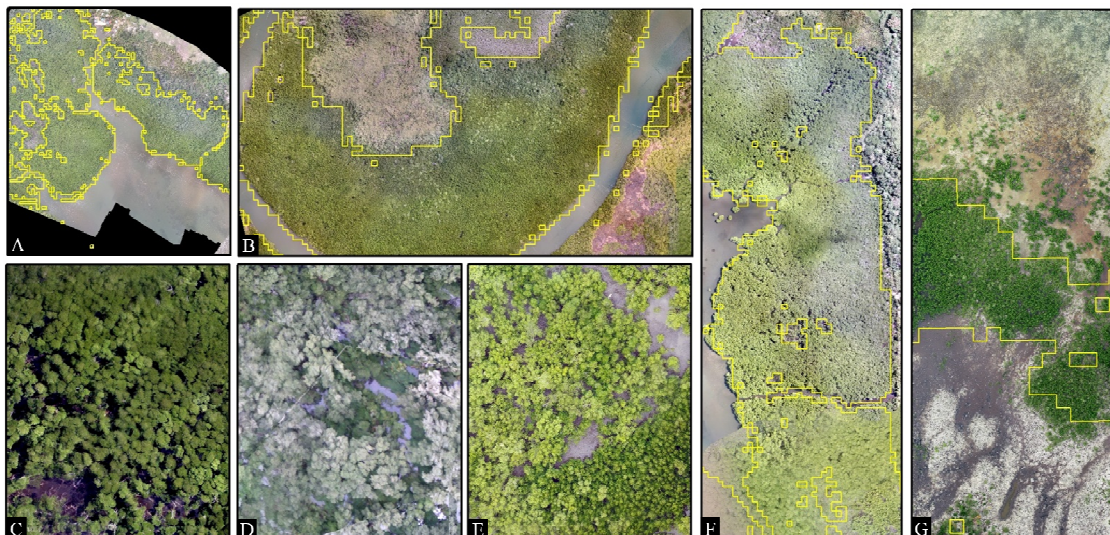


**Fig. 10.** Drone acquired orthophotos covering some of the study sites: (A) Coron, (B) Puerto Princesa, (C) Calauit Island, (D) KII Ecopark, (E) Bancal Bay, (F) Busuanga and (G) Eastern Samar. All sites have drone data except Masinloc, Zambales which was validated using mangrove field inventory. The output MVI mangrove shapefile (yellow polygons, A, B, F, and G) were overlaid in the drone images. Phantom 3, Phantom 4 and Sensefly eBee fixed wing drones were used to acquire the RGB image

The overall accuracy of MVI-derived mangrove maps as validated by high resolution drone orthophotos and field inventory data is 92% (Table 5). Ninety-four to 100% accuracy was computed for the Palawan sites: Calauit, Coron, Busuanga and Bacungan in Puerto Princesa. In Busuanga, the MVI perfectly mapped the whole mangrove extent with an accuracy of 100%. These sites are the relatively larger study sites with both sparse to dense mangrove cover. The physiographical classification of mangroves in Palawan falls under two major forest types, the fringe and riverine (Dangan-Galon et al., 2016). The validation site locations in Coron and Busuanga are within fringe mangroves, while the Calauit site is within both fringe and riverine forests. The result implies the capability of MVI to map mangroves regardless of the distance from the shore which causes variations in water salinity, tide inundation and species composition.

The index accuracy is also high for the two Iloilo sites: Banate Bay (90%) and Bancal Bay (98%). These are fringe mangroves along the bays, situated between other coastal features and the inward terrestrial vegetation. Lower accuracies were computed from